Whole-exome sequencing analysis disclosed that our patient had the *EYS* mutations, which demonstrates that the *EYS* mutations can be responsible for both the arCRD and the arRP phenotypes. Interestingly, mutations in the *ABCA4* [12–14], *CERKL* [15–18], and *C8orf37* [19, 20] genes have also been reported to be disease-causing mutations of both the arCRD and arRP phenotypes. With regard to the *ABCA4* gene mutations, the degree of functional damage caused by the various *ABCA4* mutation types can underlie the different degeneration patterns, for example, Stargardt disease (a type of macular dystrophy), arCRD or arRP [12–14]. The majority of patients with *CERKL* mutations exhibit arCRD [17, 18] and less frequently arRP [15, 16]. This is consistent with the fact that the CERKL protein is predominantly expressed in the cone photoreceptors [21]. In addition, different *C8orf37* mutations can cause either the arCRD or arRP phenotypes, which is consistent with the fact that the C8orf37 protein is expressed in both the rod and cone photoreceptors [19, 20]. However, this does not explain the pattern of the photoreceptor degeneration. On the other hand, the compound heterozygous *EYS* mutations (p.Y2935X and p.S1653KfsX2) that were found in our patient have also been reported in an arRP patient [7]. Although it is not understood why the same compound heterozygous mutations would underlie either the arCRD or arRP phenotypes, this finding suggests there is the presence of different modifier alleles between the arCRD or arRP patients with the compound heterozygous *EYS* mutations. Even so, our whole-exome sequencing analysis did not demonstrate any compound heterozygous or homozygous mutations in other 206 retinal disease-associated genes published in the RetNet database.

In conclusion, we demonstrated that *EYS* mutations are the cause of not only arRP but also arCRD. Further investigations will need to be undertaken in order to clarify the prevalence of *EYS* mutations among arCRD patients, and to determine the genotype–phenotype correlations between the arCRD and *EYS* mutations.

Acknowledgments This study was supported by grants to T.I. from the Ministry of Health, Labor and Welfare of Japan (13803661), to M.A. and T.H. from the Ministry of Education, Culture, Sports, Science and Technology of Japan (Grant-in-Aid for Scientific Research C, 25462744 and 25462738), and to T.H. from the Vehicle Racing Commemorative Foundation.

Conflict of interest The authors declare there are no conflicts of interest for this study.

References

1. Abd El-Aziz MM, Barragan I, O'Driscoll CA, Goodstadt L, Prigmore E, Borrego S, Mena M, Pieras JI, El-Ashry MF, Safieh LA, Shah A, Cheetham ME, Carter NP, Chakarova C, Ponting CP, Bhattacharya SS, Antinolo G (2008) *EYS*, encoding an ortholog of Drosophila spacemaker, is mutated in autosomal recessive retinitis pigmentosa. Nat Genet 40:1285–1287
2. Collin RW, Littink KW, Klevering BJ, van den Born LI, Koenekoop RK, Zonneveld MN, Blokland EA, Strom TM, Hoyng CB, den Hollander AI, Cremers FP (2008) Identification of a 2 Mb human ortholog of Drosophila eyes shut/spacemaker that is mutated in patients with retinitis pigmentosa. Am J Hum Genet 83:594–603
3. Abd El-Aziz MM, O'Driscoll CA, Kaye RS, Barragan I, El-Ashry MF, Borrego S, Antinolo G, Pang CP, Webster AR, Bhattacharya SS (2010) Identification of novel mutations in the ortholog of Drosophila eyes shut gene (*EYS*) causing autosomal recessive retinitis pigmentosa. Invest Ophthalmol Vis Sci 51:4266–4272
4. Audo I, Sahel JA, Mohand-Said S, Lancelot ME, Antonio A, Moskova-Doumanova V, Nandrot EF, Doumanov J, Barragan I, Antinolo G, Bhattacharya SS, Zeitz C (2010) *EYS* is a major gene for rod-cone dystrophies in France. Hum Mutat 31:E1406–E1435
5. Bandah-Rozenfeld D, Littink KW, Ben-Yosef T, Strom TM, Chowers I, Collin RW, den Hollander AI, van den Born LI, Zonneveld MN, Merin S, Banin E, Cremers FP, Sharon D (2010) Novel null mutations in the *EYS* gene are a frequent cause of autosomal recessive retinitis pigmentosa in the Israeli population. Invest Ophthalmol Vis Sci 51:4387–4394
6. Hosono K, Ishigami C, Takahashi M, Park DH, Hirami Y, Nakanishi H, Ueno S, Yokoi T, Hikoya A, Fujita T, Zhao Y, Nishina S, Shin JP, Kim IT, Yamamoto S, Azuma N, Terasaki H, Sato M, Kondo M, Minoshima S, Hotta Y (2012) Two novel mutations in the *EYS* gene are possible major causes of autosomal recessive retinitis pigmentosa in the Japanese population. PLoS ONE 7:e31036
7. Iwanami M, Oshikawa M, Nishida T, Nakadomari S, Kato S (2012) High prevalence of mutations in the *EYS* gene in Japanese patients with autosomal recessive retinitis pigmentosa. Invest Ophthalmol Vis Sci 53:1033–1040
8. Hayashi T, Gekka T, Kozaki K, Ohkuma Y, Tanaka I, Yamada H, Tsuneoka H (2012) Autosomal dominant occult macular dystrophy with an *RP1L1* mutation (R45W). Optom Vis Sci 89:684–691
9. Katagiri S, Yoshitake K, Akahori M, Hayashi T, Furuno M, Nishino J, Ikeo K, Tsuneoka H, Iwata T (2013) Whole-exome sequencing identifies a novel *ALMS1* mutation (p.Q2051X) in two Japanese brothers with Alström syndrome. Mol Vis 19:2393–2406
10. Yagasaki K, Jacobson SG (1989) Cone–rod dystrophy. Phenotypic diversity by retinal function testing. Arch Ophthalmol 107:701–708

11. Szlyk JP, Fishman GA, Alexander KR, Peachey NS, Derlacki DJ (1993) Clinical subtypes of cone–rod dystrophy. Arch Ophthalmol 111:781–788
12. Allikmets R, Singh N, Sun H, Shroyer NF, Hutchinson A, Chidambaram A, Gerrard B, Baird L, Stauffer D, Peiffer A, Rattner A, Smallwood P, Li Y, Anderson KL, Lewis RA, Nathans J, Leppert M, Dean M, Lupski JR (1997) A photoreceptor cell-specific ATP-binding transporter gene (ABCR) is mutated in recessive Stargardt macular dystrophy. Nat Genet 15:236–246
13. Klevering BJ, Yzer S, Rohrschneider K, Zonneveld M, Allikmets R, van den Born LI, Maugeri A, Hoyng CB, Cremers FP (2004) Microarray-based mutation analysis of the *ABCA4* (*ABCR*) gene in autosomal recessive cone–rod dystrophy and retinitis pigmentosa. Eur J Hum Genet 12:1024–1032
14. Klevering BJ, Deutman AF, Maugeri A, Cremers FP, Hoyng CB (2005) The spectrum of retinal phenotypes caused by mutations in the *ABCA4* gene. Graefes Arch Clin Exp Ophthalmol 243:90–100
15. Bayes M, Goldaracena B, Martinez-Mir A, Iragui-Madoz MI, Solans T, Chivelet P, Bussaglia E, Ramos-Arroyo MA, Baiget M, Vilageliu L, Balcells S, Gonzalez-Duarte R, Grinberg D (1998) A new autosomal recessive retinitis pigmentosa locus maps on chromosome 2q31–q33. J Med Genet 35:141–145
16. Tuson M, Marfany G, Gonzalez-Duarte R (2004) Mutation of *CERKL*, a novel human ceramide kinase gene, causes autosomal recessive retinitis pigmentosa (RP26). Am J Hum Genet 74:128–138
17. Auslender N, Sharon D, Abbasi AH, Garzozi HJ, Banin E, Ben-Yosef T (2007) A common founder mutation of *CERKL* underlies autosomal recessive retinal degeneration with early macular involvement among Yemenite Jews. Invest Ophthalmol Vis Sci 48:5431–5438
18. Ali M, Ramprasad VL, Soumittra N, Mohamed MD, Jafri H, Rashid Y, Danciger M, McKibbin M, Kumaramanickavel G, Inglehearn CF (2008) A missense mutation in the nuclear localization signal sequence of CERKL (p.R106S) causes autosomal recessive retinal degeneration. Mol Vis 14:1960–1964
19. Estrada-Cuzcano A, Neveling K, Kohl S, Banin E, Rotenstreich Y, Sharon D, Falik-Zaccai TC, Hipp S, Roepman R, Wissinger B, Letteboer SJ, Mans DA, Blokland EA, Kwint MP, Gijsen SJ, van Huet RA, Collin RW, Scheffer H, Veltman JA, Zrenner E, den Hollander AI, Klevering BJ, Cremers FP (2012) Mutations in *C8orf37*, encoding a ciliary protein, are associated with autosomal-recessive retinal dystrophies with early macular involvement. Am J Hum Genet 90:102–109
20. van Huet RA, Estrada-Cuzcano A, Banin E, Rotenstreich Y, Hipp S, Kohl S, Hoyng CB, den Hollander AI, Collin RW, Klevering BJ (2013) Clinical characteristics of rod and cone photoreceptor dystrophies in patients with mutations in the *C8orf37* gene. Invest Ophthalmol Vis Sci 54:4683–4690
21. Vekslin S, Ben-Yosef T (2010) Spatiotemporal expression pattern of ceramide kinase-like in the mouse retina. Mol Vis 16:2539–2549

Clinical Ophthalmology Dove

ORIGINAL RESEARCH

Retinal angiomatous proliferation associated with risk alleles of *ARMS2/HTRA1* gene polymorphisms in Japanese patients

Yasuhiro Ohkuma[1]
Takaaki Hayashi[1]
Tsutomu Sakai[1]
Akira Watanabe[1]
Hisashi Yamada[2]
Masakazu Akahori[3]
Takeshi Itabashi[3]
Takeshi Iwata[3]
Toru Noda[4]
Hiroshi Tsuneoka[1]

[1]Department of Ophthalmology, [2]Department of Molecular Genetics, Institute of DNA Medicine, The Jikei University School of Medicine, [3]Division of Molecular and Cellular Biology, National Institute of Sensory Organs, [4]Division of Ophthalmology, National Hospital Organization Tokyo Medical Center, Tokyo, Japan

Background: The purpose of this study was to investigate the association between *ARMS2/HTRA1*, *CFH*, and *C3* gene polymorphisms and retinal angiomatous proliferation (RAP), an infrequent and severe form of exudative age-related macular degeneration, which is characterized by intraretinal neovascularization.

Methods: Diagnosis of RAP was based on fundus photographs, images of fluorescein and indocyanine green angiographies, and optical coherence tomography findings. Six single nucleotide polymorphisms (SNPs), A69S (rs10490924) in *ARMS2*, rs11200638 in *HTRA1*, I62V (rs800292) in *CFH*, Y402H (rs1061170) in *CFH*, R80G (rs2230199) in *C3*, and rs2241394 in *C3*, were genotyped in eight Japanese patients with RAP.

Results: The two SNPs in the *ARMS2/HTRA1* were in complete linkage disequilibrium. The frequency of the risk T allele in *ARMS2* (the risk A allele in *HTRA1*) was 93.8% in the RAP patients. The frequency of homozygosity for the risk genotype TT of *ARMS2* (the risk genotype AA of *HTRA1*) was 87.5%. The frequency of the non-risk allele (A) of I62V was 100%. The frequencies of risk alleles of Y402H, R80G, and rs2241394 were 12.5%, 0%, and 18.8%, respectively.

Conclusion: Our results suggest that the risk alleles of the *ARMS2/HTRA1* SNPs may be associated with development of RAP and play a major role in the pathogenesis of intraretinal angiogenesis.

Keywords: age-related macular degeneration, retinal angiomatous proliferation, single nucleotide polymorphisms, *ARMS2/HTRA1* genes, components of the complement system

Introduction

Age-related macular degeneration (AMD) is the most common cause of legal blindness in the elderly, affecting more than 50 million people worldwide.[1] In Japan, the prevalence of AMD has risen from 0.87% in 1988 to 1.4% in 2007.[2,3] Maruko et al have classified exudative AMD patients into three subtypes, namely typical wet-type AMD, polypoidal choroidal vasculopathy (PCV), and retinal angiomatous proliferation (RAP).[4]

AMD is a multifactorial disease with genetic, behavioral, and environmental factors.[5] Recently, genetic association studies have revealed that single nucleotide polymorphisms (SNPs) in *CFH* (1q32), *ARMS2/HTRA1* (10q26), and *C3* (19p13) have been identified as major contributors to the pathogenesis of AMD.[6–17] Among various SNPs of those genes, the Y402H (rs1061170) and I62V (rs800292) variants in the *CFH* gene and the A69S (rs10490924) variant in the *ARMS2* gene have been investigated in detail.[6–15,18–27] The differences in genotypes associated with AMD

Correspondence: Takaaki Hayashi
Department of Ophthalmology, The Jikei University School of Medicine, 3-25-8 Nishi-shimbashi, Minato-ku, Tokyo 105-8461, Japan
Tel +81 3 3433 1111 ext 3581
Fax +81 3 3433 1936
Email taka@jikei.ac.jp

have been investigated among various ethnic groups and by subtypes of exudative AMD,[16,18–27] showing that the I62V and A69S variants are associated with AMD in both Caucasian and Asian subjects.[18–27] The Y402H and R80G (in the *C3* gene) variants have been associated with AMD in Caucasians[6–15] but not in Asians.[18,19,21–25,28] The C allele of the Y402H variant and the G allele of the R80G variant are infrequent in Asians.

The term RAP was first coined by Yannuzzi et al in 2001.[29] They suggested the retinal origin of this neovascularization, which proceeds posteriorly and finally forms a retinal-choroidal anastomosis. RAP is sometimes called type 3 neovascularization to distinguish it from type 1 neovascularization (choroidal neovascularization under the retinal pigment epithelium) and type 2 neovascularization (choroidal neovascularization that penetrates the retinal pigment epithelium).[30,31] RAP accounts for 4.5% of all exudative AMD in Japanese patients[4] and 15% of exudative AMD in Caucasian patients.[32] RAP is characterized by bilateral, multiple soft drusen, intraretinal hemorrhages, and intraretinal edema. The natural history of RAP is characterized by a rapid loss of vision.[33] RAP resists various treatments and recurs persistently.[34–40]

The phenotypic diversity of AMD is thought to be related to differences in genetic backgrounds.[20,24–27] Various reports have examined genetic backgrounds in PCV. Lee et al reported that the I62V and A69S variants, but not the Y402H variant, were related to PCV in Chinese patients.[23] Hayashi et al reported that all three of these SNPs (I62V, Y402H, and A69S) were related to PCV in Japanese patients.[26] Goto et al reported that rs2241394 in the *C3* gene was associated with PCV.[25]

Wegscheider et al reported that the Y402H polymorphism was associated with RAP in Caucasians.[20] However, the genetic association with RAP has not been evaluated sufficiently because of the rarity of RAP in Japan. There are only a few reports about associations between A69S and RAP in the Japanese population.[26,27] The purpose of the current study was to investigate the involvement of genetic factors in not only the *ARMS2/HTRA1* but also the *CFH* and *C3* genes in Japanese patients with RAP.

Materials and methods

The study was approved by the institutional review board of The Jikei Medical University, and all procedures were conducted in accordance with the principles of the Declaration of Helsinki. Eight unrelated Japanese patients with RAP were recruited from the Department of Ophthalmology at The Jikei Medical University and the National Hospital Organization Tokyo Medical Center. Informed consent was obtained from all subjects.

All patients with RAP underwent a full ophthalmic examination, including slit-lamp biomicroscopy, funduscopy, optical coherence tomography, and fluorescein and indocyanine green fundus angiographies. The diagnosis of RAP was based on the criteria of Yannuzzi et al[29] and was classified as a defined anastomosis connecting the retinal circulation to a vascular complex within the retina, usually with surrounding intraretinal blood and intraretinal or cystoid macular edema.

Genomic DNA was extracted from the peripheral blood of each individual. A total of six SNPs consisting of A69S (rs10490924) in *ARMS2*, rs11200638 in *HTRA1*, Y402H (rs1061170) in *CFH*, I62V (rs800292) in *CFH*, R80G (rs2230199) in *C3*, and rs2241394 in *C3* were genotyped. Polymerase chain reaction amplification was performed using LA Taq polymerase (Takara Bio Inc, Ohtsu, Japan) and primers for *ARMS2* (forward primer: 5′-GCCTATACCCAGGACCGATG-3′, reverse primer: 5′-CATGTTCTCAGCATCTCCAAGTC-3′), *HTRA1* (forward primer: 5′-TCTCTGCGAATACGGACACG-3′, reverse primer: 5′-ACT GTG TCCATT CAG CTC CTA A-3′), *CFH* Y402H (forward primer: 5′-CAGAAATAGGGCCAAGAAAAGAGT-3′, reverse primer: 5′-ATGTAACTGTGGTCTGCGC-3′), *CFH* I62V (forward primer: 5′-GATTGCAATGAACTTCCTCCAAG-3′, reverse primer: 5′-GGATTAAGAGCAACC CATTCTCC-3′), *C3* R80G (forward primer: 5′-CCTCGCACCTCCTTCACA-3′, reverse primer: 5′-TCTGGCTGGCACCTCAAT-3′), and *C3* rs2241394 (forward primer: 5′-GGCTGGGTGACTGTACCTCTTC-3′, reverse primer: 5′-CATGTTCTCAGCATCTCCAAGTC-3′) to amplify these regions. Polymerase chain reaction products were used as the templates for direct DNA sequencing kits (Applied Biosystems, Foster City, CA, USA) on an automated sequencer (3730xl DNA analyzer; Applied Biosystems).

Results

Genetic analysis

Five men and three women were analyzed in the study. The mean patient age was 82.6±4.6 years (range 76–91 years). Both eyes were affected in four patients (50.0%). All SNPs were successfully genotyped in all patients (Table 1). The two SNPs in the *ARMS2/HTRA1* were in complete linkage disequilibrium. The frequency of the risk T allele in

Table 1 Polymorphisms in *ARMS2/HTRA1/CFH/C3* genes: genotypes in Japanese patients with retinal angiomatous proliferation

Patient number	Age	Sex	Affected eye	*ARMS2*	*HTRA1*	*CFH*		*C3*	
				rs10490924 (A69S)	rs1120638	rs800292 (I62V)	rs1061170 (Y402H)	rs2230199 (R80G)	rs2241394
1	83	F	Bilateral	**TT**	**AA**	AA	TT	CC	**CG**
2	79	M	Unilateral	**TT**	**AA**	AA	**CT**	CC	CC
3	84	M	Unilateral	**TT**	**AA**	AA	TT	CC	CC
4	87	F	Unilateral	**TT**	**AA**	AA	**CT**	CC	**CG**
5	82	M	Bilateral	**TT**	**AA**	AA	TT	CC	CC
6	78	M	Unilateral	**TT**	**AA**	AA	TT	CC	CC
7	76	F	Bilateral	**TT**	**AA**	AA	TT	CC	**CG**
8	91	M	Bilateral	**TG**	**AG**	AA	TT	CC	CC

Note: Risk alleles are shown in bold.
Abbreviations: M, male; F, female.

the *ARMS2* gene (the risk A allele in the *HTRA1* gene) was 93.8%. The frequency of homozygosity for the risk genotype (TT) of the *ARMS2* gene was 87.5%. The frequency of the non-risk allele (A) of I62V was 100%. The frequencies of risk alleles of Y402H in the *CFH* gene, rs2230199 (R80G) and rs2241394 in the *C3* gene were 12.5%, 0%, and 18.8%, respectively.

Representative case (patient 1)

An 83-year-old woman with homozygosity for the risk genotype (TT) of the *ARMS2* gene presented with bilateral RAP (Figure 1). She had undergone cataract surgery in both eyes prior to diagnosis of RAP. Her decimal best-corrected visual acuity was 0.3 in the right eye and 0.07 in the left eye. Both eyes were treated by standard-fluence photodynamic therapy with verteporfin (Visudyne®, Novartis Pharma AG, Basel, Switzerland) in combination with 1.25 mg (0.05 mL) of intravitreal bevacizumab (Avastin®, Genentech, San Francisco, CA, USA), and her vision improved to 0.5 in the right eye and 0.15 in the left eye, with a rapid resolution of intraretinal edema. There was no recurrence of intraretinal edema or hemorrhages, and her vision remained stable for 2 years following the combination therapy.

Discussion

In this study we genotyped six SNPs in RAP patients that were highly representative of the common genetic variations of exudative AMD. Our results raise the possibility of an association between *ARMS2* (A69S)/*HTRA1* (rs1120638) variants and RAP, but a weak association for the other SNPs. Hayashi et al recently demonstrated that the A69S, Y402H, and I62V variants are associated with RAP and that the A69S variant has the strongest association for RAP among the three exudative AMD subtypes.[26] Tanaka et al also reported that A69S might serve as strong genetic markers of RAP.[27] Our findings are consistent with their findings[26,27] regarding the A69S variant, but we had negative results for the I62V (*CFH*) variant (Table 2).

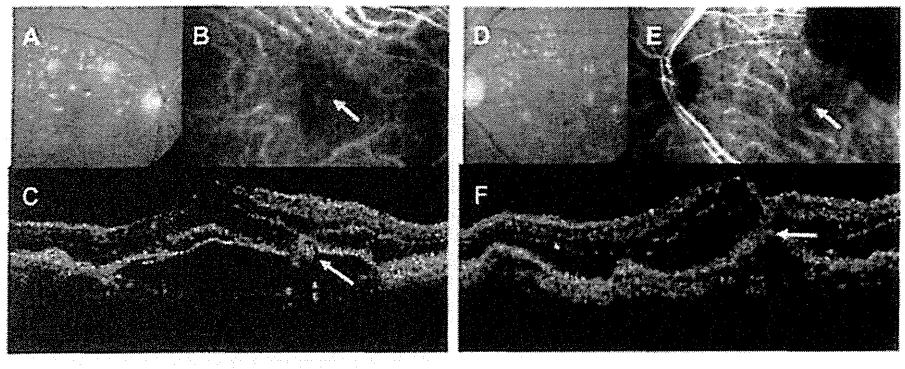

Figure 1 Color fundus photographs (**A** and **D**), indocyanine green fundus angiographies (**B** and **E**), and optical coherence tomography images (**C** and **F**) from the right eye (**A–C**) and the left eye (**D–F**) of an 83-year-old woman (patient 1).
Notes: We diagnosed her right eye with stage II retinal angiomatous proliferation and her left eye with stage III retinal angiomatous proliferation. (**A** and **D**) Fundus image shows intraretinal hemorrhages with a large number of soft drusen and pigment epithelial detachment. (**B**) Indocyanine green fundus angiographies shows some hotspots. One of them connects retinal vessels (arrow), corresponding to the intraretinal neovascularization. (**C**) A vertical optical coherence tomography image shows a pigment epithelial detachment, cystoid macular edema, and retinal angiomatous proliferation lesion (arrow). (**E**) Indocyanine green fundus angiographies shows choroidal neovascularization (arrow) that connects retinal vessels, corresponding to retinal-choroidal anastomosis. (**F**) A vertical optical coherence tomography image shows a pigment epithelial detachment, cystoid macular edema, and a retinal pigment epithelium line that has ruptured (arrow).

Table 2 Genotype frequency of A69S (*ARMS2*), I62V (*CFH*), and Y402H (*CFH*) polymorphisms in Japanese controls and Japanese patients with retinal angiomatous proliferation

Genotype	rs10490924 (A69S)			rs800292 (I62V)			rs1061170 (Y402H)		
	TT	TG	GG	GG	GA	AA	CC	CT	TT
Controls (n=1,351)[26]	196 (14.6%)	638 (47.8%)	502 (37.6%)	456 (34.1%)	649 (48.5%)	233 (17.4%)	8 (0.6%)	160 (11.9%)	1,174 (87.5%)
Patients (n=36)[26]	31 (86.1%)	3 (8.3%)	2 (5.6%)	20 (55.6%)	11 (30.6%)	5 (13.8%)	0 (0%)	5 (14.3%)	30 (85.7%)
Patients (n=51)[27]	39 (76.5%)	10 (19.6%)	2 (3.9%)	29 (56.9%)	20 (39.2%)	2 (3.9%)	ND	ND	ND
Patients (n=8) (in present study)	7 (87.5%)	1 (12.5%)	0 (0%)	0 (0%)	0 (0%)	8 (100%)	0 (0%)	2 (25%)	6 (75%)

Note: Risk alleles are shown in **bold**.
Abbreviation: ND, not described.

Components of the complement system have been identified in drusen, indicating a potential role of the complement system in the pathogenesis of AMD.[41,42] C3 and CFH are key components of the alternative complement pathway. C3 is the most abundant complement component and is synthesized predominantly in the liver. Cleavage of C3 into C3a and C3b is the central step in complement activation and can be initiated by the classic antibody-mediated pathway, the lectin pathway, or the alternative complement pathway. CFH is a critical negative regulator of the alternative pathway of the complement system. It binds to C3b, promotes the decay of C3 convertase, and serves as a cofactor for the factor I-mediated proteolytic inactivation of C3b, resulting in inhibition of the complement cascade.

Because there are bilateral multiple soft drusen in the presence in RAP, we suspected that RAP would be more strongly associated with genetic abnormalities in the complement system than other AMD subtypes. However, we hardly detected the risk alleles of the *CFH* and *C3* genes. One reason for these results is the infrequency of the C allele in Y402H and the G allele in R80G in Asians. Reticular pseudodrusen (RPD) are defined as "drusen that form ill-defined networks of broad interlacing ribbons" in the Wisconsin grading system for maculopathy.[43] RPD have been recognized as a distinctive morphologic feature observed in exudative AMD.[44] Recent studies have demonstrated the association between RPD and reduced macular sensitivity.[45,46] Importantly, it is reported that the prevalence of RPD was high in patients with RAP and the risk genotype (TT) in A69S,[47] and RPD usually occurs bilaterally,[48] suggesting the impact of genetic background for RPD.

It was an unexpected result that we did not detect the risk G allele in I62V (Table 2). The I62V variant has been associated with exudative AMD in both Caucasian and Asian patients.[18,19,21–25,27] In Japanese population samples, it has been demonstrated that the risk genotype (GG) in I62V is significantly associated with RAP (Table 2).[26,27] However, the risk genotype in I62V was not detected in our RAP patients (Table 2). Our findings suggest that the presence of the risk genotype (I62V) may not be necessarily associated with development of RAP. A larger sample size will be required to determine whether the risk genotype in I62V is eventually associated with RAP.

RAP is characterized by intraretinal neovascularization above the retinal pigment epithelium. Two different origins of this neovascularization have been proposed. Yannuzzi et al suggested that the neovascularization in RAP originates from the neural retina.[29] On the other hand, Freund et al proposed type 3 neovascularization that originates not only from deep retinal capillaries but also from the choroid.[31] As for the location of gene expression, the *CFH* gene is expressed primarily in the retinal pigment epithelium, drusen, and choroidal capillaries;[6] the *C3* gene is expressed in the neural retina, choroid, and retinal pigment epithelium;[41] and the *ARMS2* gene is expressed in the ellipsoid region of the photoreceptor cells.[14] Since it seems that the location of characteristic neovascularization corresponds to the location of susceptible gene expression in RAP, our results support the hypothesis by Yannuzzi et al[29] that the origin of neovascularization in RAP is in the neural retina.

In conclusion, our results suggest that the risk alleles/genotypes of the *ARMS2/HTRA1* SNPs may be strongly associated with development of RAP and that they play a major role in the pathogenesis of intraretinal angiogenesis.

Acknowledgments

This work was supported by grants from The Jikei University Research Fund (TH) and the Vehicle Racing Commemorative Foundation (TH and HT).

Disclosure

The authors report no conflicts of interest in this work.

References

1. Klein R, Peto T, Bird A, Vannewkirk MR. The epidemiology of age-related macular degeneration. *Am J Ophthalmol*. 2004;137(3):486–495.
2. Oshima Y, Ishibashi T, Murata T, Tahara Y, Kiyohara Y, Kubota T. Prevalence of age related maculopathy in a representative Japanese population: the Hisayama study. *Br J Ophthalmol*. 2001;85(10):1153–1157.
3. Yasuda M, Kiyohara Y, Hata Y, et al. Nine-year incidence and risk factors for age-related macular degeneration in a defined Japanese population the Hisayama study. *Ophthalmology*. 2009;116(11):2135–2140.
4. Maruko I, Iida T, Saito M, Nagayama D, Saito K. Clinical characteristics of exudative age-related macular degeneration in Japanese patients. *Am J Ophthalmol*. 2007;144(1):15–22.
5. de Jong PT. Age-related macular degeneration. *N Engl J Med*. 2006;355(14):1474–1485.
6. Klein RJ, Zeiss C, Chew EY, et al. Complement factor H polymorphism in age-related macular degeneration. *Science*. 2005;308(5720):385–389.
7. Haines JL, Hauser MA, Schmidt S, et al. Complement factor H variant increases the risk of age-related macular degeneration. *Science*. 2005;308(5720):419–421.
8. Edwards AO, Ritter R 3rd, Abel KJ, Manning A, Panhuysen C, Farrer LA. Complement factor H polymorphism and age-related macular degeneration. *Science*. 2005;308(5720):421–424.
9. Maller J, George S, Purcell S, et al. Common variation in three genes, including a noncoding variant in CFH, strongly influences risk of age-related macular degeneration. *Nat Genet*. 2006;38(9):1055–1059.
10. Li M, Atmaca-Sonmez P, Othman M, et al. CFH haplotypes without the Y402H coding variant show strong association with susceptibility to age-related macular degeneration. *Nat Genet*. 2006;38(9):1049–1054.
11. Hughes AE, Orr N, Esfandiary H, Diaz-Torres M, Goodship T, Chakravarthy U. A common CFH haplotype, with deletion of CFHR1 and CFHR3, is associated with lower risk of age-related macular degeneration. *Nat Genet*. 2006;38(10):1173–1177.
12. Dewan A, Liu M, Hartman S, et al. HTRA1 promoter polymorphism in wet age-related macular degener ation. *Science*. 2006;314(5801):989–992.
13. Yang Z, Camp NJ, Sun H, et al. A variant of the HTRA1 gene increases susceptibility to age-related macular degeneration. *Science*. 2006;314(5801):992–993.
14. Fritsche LG, Loenhardt T, Janssen A, et al. Age-related macular degeneration is associated with an unstable ARMS2 (LOC387715) mRNA. *Nat Genet*. 2008;40(7):892–896.
15. Kanda A, Chen W, Othman M, et al. A variant of mitochondrial protein LOC387715/ARMS2, not HTRA1, is strongly associated with age-related macular degeneration. *Proc Natl Acad Sci U S A*. 2007;104(41):16227–16232.
16. Spencer KL, Olson LM, Anderson BM, et al. C3 R102G polymorphism increases risk of age-related macular degeneration. *Hum Mol Genet*. 2008;17(12):1821–1824.
17. Edwards AO, Fridley BL, James KM, Sharma AK, Cunningham JM, Tosakulwong N. Evaluation of clustering and genotype distribution for replication in genome wide association studies: the age-related eye disease study. *PLoS One*. 2008;3(11):e3813.
18. Chen LJ, Liu DT, Tam PO, et al. Association of complement factor H polymorphisms with exudative age-related macular degeneration. *Mol Vis*. 2006;12:1536–1542.
19. Mori K, Gehlbach PL, Kabasawa S, et al. Coding and noncoding variants in the CFH gene and cigarette smoking influence the risk of age-related macular degeneration in a Japanese population. *Invest Ophthalmol Vis Sci*. 2007;48(11):5315–5319.
20. Wegscheider BJ, Weger M, Renner W, et al. Association of complement factor H Y402H gene polymorphism with different subtypes of exudative age-related macular degeneration. *Ophthalmology*. 2007;114(4):738–742.
21. Kim NR, Kang JH, Kwon OW, Lee SJ, Oh JH, Chin HS. Association between complement factor H gene polymorphisms and neovascular age-related macular degeneration in Koreans. *Invest Ophthalmol Vis Sci*. 2008;49(5):2071–2076.
22. Ng TK, Chen LJ, Liu DT, et al. Multiple gene polymorphisms in the complement factor h gene are associated with exudative age-related macular degeneration in chinese. *Invest Ophthalmol Vis Sci*. 2008;49(8):3312–3317.
23. Lee KY, Vithana EN, Mathur R, et al. Association analysis of CFH, C2, BF, and HTRA1 gene polymorphisms in Chinese patients with polypoidal choroidal vasculopathy. *Invest Ophthalmol Vis Sci*. 2008;49(6):2613–2619.
24. Kondo N, Honda S, Kuno S, Negi A. Coding variant I62V in the complement factor H gene is strongly associated with polypoidal choroidal vasculopathy. *Ophthalmology*. 2009;116(2):304–310.
25. Goto A, Akahori M, Okamoto H, et al. Genetic analysis of typical wet-type age-related macular degeneration and polypoidal choroidal vasculopathy in Japanese population. *J Ocul Biol Dis Infor*. 2009;2(4):164–175.
26. Hayashi H, Yamashiro K, Gotoh N, et al. CFH and ARMS2 variations in age-related macular degeneration, polypoidal choroidal vasculopathy, and retinal angiomatous proliferation. *Invest Ophthalmol Vis Sci*. 2010;51(11):5914–5919.
27. Tanaka K, Nakayama T, Yuzawa M, et al. Analysis of candidate genes for age-related macular degeneration subtypes in the Japanese population. *Mol Vis*. 2011;17:2751–2758.
28. Pei XT, Li XX, Bao YZ, et al. Association of c3 gene polymorphisms with neovascular age-related macular degeneration in a Chinese population. *Curr Eye Res*. 2009;34(8):615–622.
29. Yannuzzi LA, Negrao S, Iida T, et al. Retinal angiomatous proliferation in age-related macular degeneration. *Retina*. 2001;21(5):416–434.
30. Gass JD. Biomicroscopic and histopathologic considerations regarding the feasibility of surgical excision of subfoveal neovascular membranes. *Am J Ophthalmol*. 1994;118(3):285–298.
31. Freund KB, Ho IV, Barbazetto IA, et al. Type 3 neovascularization: the expanded spectrum of retinal angiomatous proliferation. *Retina*. 2008;28(2):201–211.
32. Cohen SY, Creuzot-Garcher C, Darmon J, et al. Types of choroidal neovascularisation in newly diagnosed exudative age-related macular degeneration. *Br J Ophthalmol*. 2007;91(9):1173–1176.
33. Viola F, Massacesi A, Orzalesi N, Ratiglia R, Staurenghi G. Retinal angiomatous proliferation: natural history and progression of visual loss. *Retina*. 2009;29(6):732–739.
34. Slakter JS, Yannuzzi LA, Schneider U, et al. Retinal choroidal anastomoses and occult choroidal neovascularization in age-related macular degeneration. *Ophthalmology*. 2000;107(4):742–753.
35. Kuroiwa S, Arai J, Gaun S, Iida T, Yoshimura N. Rapidly progressive scar formation after transpupillary thermotherapy in retinal angiomatous proliferation. *Retina*. 2003;23(3):417–420.
36. Boscia F, Furino C, Sborgia L, Reibaldi M, Sborgia C. Photodynamic therapy for retinal angiomatous proliferations and pigment epithelium detachment. *Am J Ophthalmol*. 2004;138(6):1077–1079.
37. Bottoni F, Massacesi A, Cigada M, Viola F, Musicco I, Staurenghi G. Treatment of retinal angiomatous proliferation in age-related macular degeneration: a series of 104 cases of retinal angiomatous proliferation. *Arch Ophthalmol*. 2005;123(12):1644–1650.
38. Sakimoto S, Gomi F, Sakaguchi H, Tano Y. Recurrent retinal angiomatous proliferation after surgical ablation. *Am J Ophthalmol*. 2005;139(5):917–918.
39. Shiragami C, Iida T, Nagayama D, Baba T, Shiraga F. Recurrence after surgical ablation for retinal angiomatous proliferation. *Retina*. 2007;27(2):198–203.
40. Silva RM, Cachulo ML, Figueira J, de Abreu JR, Cunha-Vaz JG. Chorioretinal anastomosis and photodynamic therapy: a two-year follow-up study. *Graefes Arch Clin Exp Ophthalmol*. 2007;245(8):1131–1139.
41. Mullins RF, Russell SR, Anderson DH, Hageman GS. Drusen associated with aging and age-related macular degeneration contain proteins common to extracellular deposits associated with atherosclerosis, elastosis, amyloidosis, and dense deposit disease. *FASEB J*. 2000;14(7):835–846.

42. Johnson LV, Leitner WP, Staples MK, Anderson DH. Complement activation and inflammatory processes in Drusen formation and age related macular degeneration. *Exp Eye Res*. 2001;73(6):887–896.
43. Klein R, Davis MD, Magli YL, Segal P, Klein BE, Hubbard L. The Wisconsin age-related maculopathy grading system. *Ophthalmology*. 1991;98(7):1128–1134.
44. Cohen SY, Dubois L, Tadayoni R, Delahaye-Mazza C, Debibie C, Quentel G. Prevalence of reticular pseudodrusen in age-related macular degeneration with newly diagnosed choroidal neovascularisation. *Br J Ophthalmol*. 2007;91(3):354–359.
45. Ooto S, Ellabban AA, Ueda-Arakawa N, et al. Reduction of retinal sensitivity in eyes with reticular pseudodrusen. *Am J Ophthalmol*. 2013;156(6):1184–1191.
46. Querques G, Massamba N, Srour M, Boulanger E, Georges A, Souied EH. Impact of reticular pseudodrusen on macular function. *Retina*. July 9, 2013. [Epub ahead of print.]
47. Ueda-Arakawa N, Ooto S, Nakata I, et al. Prevalence and genomic association of reticular pseudodrusen in age-related macular degeneration. *Am J Ophthalmol*. 2013;155(2):260–269.
48. Lee MY, Yoon J, Ham DI. Clinical characteristics of reticular pseudodrusen in Korean patients. *Am J Ophthalmol*. 2012;153(3):530–535.

Molecular Vision 2013; 19:2393-2406 <http://www.molvis.org/molvis/v19/2393>
Received 11 September 2013 | Accepted 22 November 2013 | Published 24 November 2013

Whole-exome sequencing identifies a novel *ALMS1* mutation (p.Q2051X) in two Japanese brothers with Alström syndrome

Satoshi Katagiri,[1,2] Kazutoshi Yoshitake,[3] Masakazu Akahori,[1] Takaaki Hayashi,[2] Masaaki Furuno,[4] Jo Nishino,[3] Kazuho Ikeo,[3] Hiroshi Tsuneoka,[2] Takeshi Iwata[1]

[1]Division of Molecular and Cellular Biology, National Institute of Sensory Organs, National Hospital Organization Tokyo Medical Center, Tokyo, Japan; [2]Department of Ophthalmology, The Jikei University School of Medicine, Tokyo, Japan; [3]Laboratory of DNA Data Analysis, National Institute of Genetics, Shizuoka, Japan; [4]RIKEN Center for Life Science Technologies, Division of Genomic Technologies, Life Science Accelerator Technology Group, Transcriptome Technology Team, Yokohama, Japan

Purpose: No mutations associated with Alström syndrome (AS), a rare autosomal recessive disease, have been reported in the Japanese population. The purpose of this study was to investigate the genetic and clinical features of two brothers with AS in a consanguineous Japanese family.

Methods: Whole-exome sequencing analysis was performed on two brothers with AS and their unaffected parents. We performed a complete ophthalmic examination, including decimal best-corrected visual acuity, slit-lamp and funduscopic examination, visual-field and color-vision testing, full-field electroretinography, and optical coherence tomography. Fasting blood tests and systemic examinations were also performed.

Results: A novel mutation (c.6151C>T in exon 8) in the Alström syndrome 1 (*ALMS1*) gene that causes a premature termination codon at amino acid 2051 (p.Q2051X), was identified in the homozygous state in the affected brothers and in the heterozygous state in the parents. The ophthalmologic findings for both brothers revealed infantile-onset severe retinal degeneration and visual impairment, marked macular thinning, and severe cataracts. Systemic findings showed hepatic dysfunction, hyperlipidemia, hypogonadism, short stature, and wide feet in both brothers, whereas hearing loss, renal failure, abnormal digits, history of developmental delay, scoliosis, hypertension, and alopecia were not observed in either brother. The older brother exhibited type 2 diabetic mellitus and obesity, whereas the younger brother had hyperinsulinemia and subclinical hypothyroidism.

Conclusions: A novel *ALMS1* mutation was identified by using whole-exome sequencing analysis, which is useful not only to identify a disease causing mutation but also to exclude other gene mutations. Although characteristic ophthalmologic findings and most systemic findings were similar between the brothers, the brothers differed slightly in terms of glucose tolerance and thyroid function.

Alström syndrome (AS; OMIM: 203800) is a rare and autosomal recessive hereditary disease with an estimated prevalence of less than 0.001% [1,2]. AS is caused by mutations in the *ALMS1* gene, which is located on chromosome 2p13 [3,4]. ALMS1 is localized to centrosomes and ciliary basal bodies [5,6] and has been implicated in the function, formation, and maintenance of primary cilia [5,7–9]. Dysfunction of primary cilia caused by mutations in genes such as *ALMS1* leads to a multitude of human monogenic disorders known as ciliopathies [10,11]; these include plural systemic diseases, such as AS, Usher syndrome, Bardet–Biedl syndrome (BBS), Senior–Løken syndrome, Joubert syndrome, Meckel–Gruber syndrome, and orofaciodigital syndrome 1 [11,12]. The majority of *ALMS1* mutations are nonsense and frameshift variations (primarily clustered in exons 8, 10, and 16) that are predicted to cause truncated proteins [3,4,13]. In the photoreceptors, *ALMS1* mutations lead to defective function of the connecting cilium.

AS is characterized by a wide spectrum of disorders, such as early onset severe retinal degeneration, obesity from childhood, hyperinsulinemia, type 2 diabetic mellitus (T2DM), hepatic dysfunction, heart failure, sensory hearing loss, and renal failure [14]. Other manifestations include acanthosis nigricans, alopecia, hypogonadism, hypothyroidism, hyperlipidemia, short stature, and scoliosis [15,16]. In most cases of AS, cone–rod degeneration in the first decade, normal intelligence, and no polydactyly serve as a differential diagnosis of BBS, which exhibits similar clinical findings to AS [17].

Almost all patients with AS show nystagmus and severe photophobia from infancy [14,18]. Visual impairment is usually seen at an age younger than 1 year [18]. Although the rate of progression of vision loss is variable, all patients

Correspondence to: Takaaki Hayashi, Department of Ophthalmology, The Jikei University School of Medicine, 3-25-8, Nishi-shimbashi, Minato-ku, Tokyo, 105-8461, Japan; Phone: +81-3-3433-1111 (ext. 3581); FAX: +81-3-5378-8828; email: taka@jikei.ac.jp

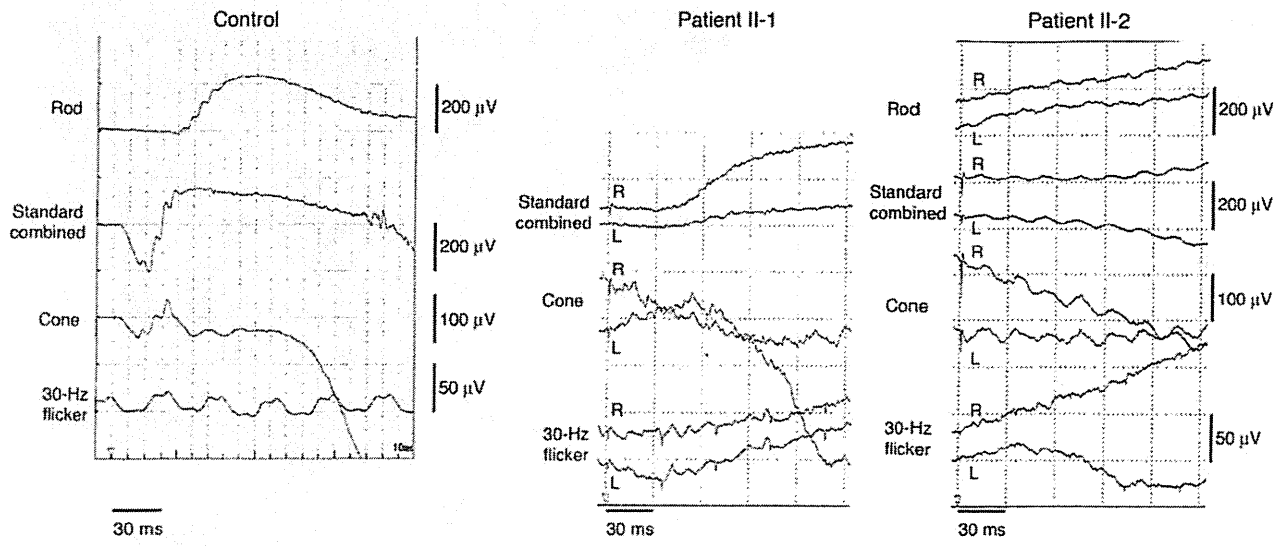

Figure 2. Full-field electroretinogram. The electroretinograms (ERGs; patient II-1) at the age of 9 years, showing no standard combined, photopic, or 30-Hz flicker responses in either eye. The ERGs (patient II-2) at the age of 7 years, showing no rod, standard combined, photopic, or 30-Hz flicker responses in either eye.

Clinical Electrophysiology of Vision. The procedure and conditions for ERG recording have been detailed previously [33].

Fasting venous blood samples were analyzed for glucose, lipid, lipoprotein, and hemogram levels and renal, liver, and thyroid function tests. In addition, hemoglobin A_{1c}, insulin, anti-thyroid peroxidase, anti-thyroglobulin antibodies, cortisol, luteinizing hormone, follicle stimulating hormone, testosterone, estradiol, prolactin, parathyroid hormone, and thyroid receptor antibody levels were examined. Chest X-rays and electrocardiograms were also performed.

DNA preparation and exome sequencing analysis: We obtained venous blood samples from the affected brothers and their unaffected parents. Genomic DNA was extracted from the blood samples by using a Gentra Puregene Blood kit (Qiagen, Tokyo, Japan) and sheared with a Covaris Ultrasonicator (Covaris, Woburn, MA). Construction of paired-end sequence libraries and exome capture were performed by using the Agilent Bravo automated liquid-handling platform with SureSelect XT Human All Exon kit V4 + UTRs kit (Agilent Technologies, Santa Clara, CA) according to the manufacturer's instructions. Enriched libraries were sequenced by using in Illumina HiSeq2000 sequencer (San Diego, CA), according to the manufacturer's instructions for 100-bp paired-end sequencing. Reads were mapped to the reference human genome (1000 genomes phase 2 reference, hs37d5) with Burrows–Wheeler Aligner software version 0.6.2 [34]. Duplicated reads were then removed by Picard MarkDuplicates module version 1.62, and mapped reads around insertion–deletion polymorphisms (INDELs) were realigned by using the Genome Analysis Toolkit (GATK) version 2.1–13 [35]. Base-quality scores were recalibrated by using GATK. Calling of mutations was performed by using the GATK UnifiedGenotyper module, and called single-nucleotide variants and INDELs were annotated by using snpEff software version 3.0 [36]. The mutations were annotated with the snpEff score ("HIGH," "MODERATE," or "LOW") and with the allele frequency in the 1000 genomes database. The mutations were then filtered so that only those with "HIGH" or "MODERATE" snpEff scores (indicating that the amino acid sequence would be functionally affected) and a frequency of less than 1% in the 1000 genome database were analyzed further. We also used new variations, which were not found in the in-house database of seven people exome data with control individuals without ocular diseases. Mutations were classified by hereditary information into homozygous recessive, heterozygous recessive, and de novo mutations in the family members. Filtered mutations were scored with PolyPhen software version 2.2.2 [37], which predicts the effect on the structure and function of the protein. The above exome analysis pipeline is available at Cell Innovation.

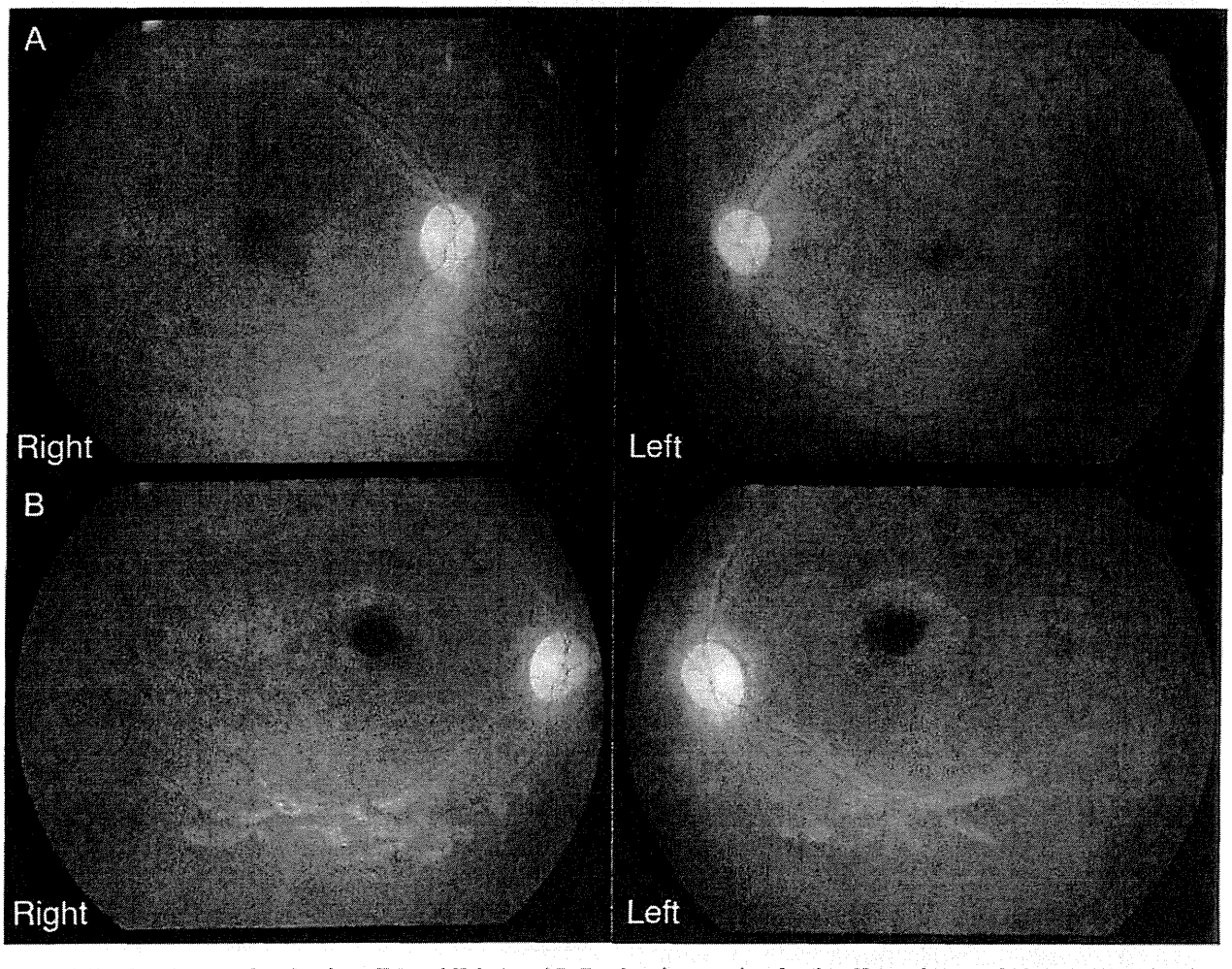

Figure 4. Fundus photographs of patients II-1 and II-2. **A** and **B**: Fundus photographs of patient II-1 at the age of 14 years (**A**) and patient II-2 at the age of 8 years (**B**) show retinal degeneration with attenuated vessels in the posterior poles of both eyes.

combined, photopic, or 30-Hz flicker responses in either eye (Figure 2). GP analysis at the age of 11 years showed markedly constricted visual fields in V-4e and I-4e isopters of both eyes (Figure 3A). The fundus photographs at the age of 14 years showed retinal degeneration with attenuated vessels from the arcade to the periphery in both eyes (Figure 4A). GP analysis at the age of 16 years showed more marked constricted visual fields of V-4e and I-4e isopters in both eyes than those observed at the age of 11 years (Figure 3B); a similar analysis at the age of 22 years showed a small visual field of V-4e isopter in the right eye and no visual field in the left eye (Figure 3C). TD-OCT at the age of 22 years showed total macular thinning in both eyes (Figure 5A). At the age of 29 years, his BCVA was light perception (LP) in the right eye and no light perception in the left eye. Intraocular pressure in each eye was within the normal range. He had severe cortical and subcapsular cataracts in the right (Figure 6) and left eyes, and the fundi were not visible due to these cataracts.

Ophthalmologic findings for patient II-2: Patient II-2, the younger of the two brothers, visited our hospital at the age of 2 years and 6 months with the main complaint of poor visual acuity and photophobia. At the age of 3 years, his BCVA was 0.01 (+1.50 dpt) in the right eye and 0.01 (+1.50 dpt) in the left eye. Fundus examination showed retinal degeneration with slight attenuation of peripheral vessels. At the age of 4 years, he failed the Ishihara test. At the age of 6 years, the panel D-15 test showed irregular arrangements along no particular axis, and the GP could not be measured well because of low visual acuity and nystagmus. The ERG at the age of 7 years showed no rod, standard combined, photopic, or 30-Hz flicker responses in either eye (Figure 2). The fundus examination at

Figure 6. Anterior segment of the right eye in patient II-1. A severe cortical and anterior subcapsular cataract is present at the age of 29 years.

Systemic features except ocular findings: Systemic examinations were performed for patient II-1 at the age of 29 and patient II-2 at the age of 23. Both patients had hepatic dysfunction, hyperlipidemia, hypogonadism, short stature, and flat feet, and neither patient had hearing loss, renal failure, abnormal digits, history of developmental delay, mental retardation, scoliosis, hypertension, or alopecia. Obesity was present in patient II-1 only. Patient II-1 had T2DM, whereas patient II-2 showed hyperinsulinemia. Subclinical hypothyroidism was diagnosed in patient II-2 only. Recurrent pulmonary infections were not observed, and chest X-rays showed neither fibrotic infiltrations nor cardiac dilation in either patient. Infantile asthma was experienced by both patients. Electrocardiogram analysis showed no arrhythmia in either patient. Summaries of the clinical features, bio-information, and detailed laboratory data are presented in Table 1 and Table 2. Collectively, the phenotypes of the brothers were consistent with those described for AS.

Exome sequencing analysis and identification of a gene mutation: We performed whole-exome sequencing of the two affected brothers and their parents by using the Agilent SureSelect Human All Exon kit followed by Illumina HiSeq 2000 platforms. Sequences of average length 11.8 Gb were generated from 101-bp paired-end sequences. After eliminating reads from PCR duplicates by discarding reads with duplicated start sites, we achieved 58-fold depth and 87% coverage in Refseq annotated regions (Table 3). When the sequences were compared with the reference human genome (hs37d5), 3,506,741 mutations were found in the two brothers and their parents (Table 4). To distinguish potentially causal mutations from other mutations, we focused only on mutations that could change the amino acid sequence (19,574 mutations), such as nonsynonymous mutations, splice acceptor and donor site mutations, and INDELs. We also assumed the frequency of the mutations responsible for AS is likely to be under 1%. After filtering with snpEff score and frequency criteria, we filtered the remaining 3,685 mutations by using the pattern of inheritance and identified 17 gene mutations as causal candidates. Among these mutations, nine mutations were found homozygous in the HECT domain containing E3 ubiquitin protein ligase 3 (*HECTD3*), the vitrin (*VIT*), the protein kinase domain containing, cytoplasmic (*PKDCC*), the ATP-binding cassette, sub-family G (*WHITE*), member 8 (*ABCG8*), the leucine-rich pentatricopeptide repeat containing (*LRPPRC*), the G protein-coupled receptor 75 (*GPR75*), the notochord homeobox (*NOTO*), the matrix-remodelling associated 5 (*MXRA5*), and the *ALMS1* genes. Eight mutations were found as compound heterozygous mutations within the PERP, TP53 apoptosis effector (*PERP*), the transforming, acidic coiled-coil containing protein 2 (*TACC2*), the zinc finger protein, FOG family member 1 (*ZFPM1*), and the lipoxygenase homology domains 1 (*LOXHD1*) genes. No de novo mutations were found. To determine the causative gene, we investigated SAGE (EyeSAGE) database to determine if the candidate genes are expressed in the retina. Nine candidate mutations were identified within *VIT, LRPPRC, PERP, TACC2, ZFPM1,* and *ALMS1* genes. These nine candidate genes were further reduced by the BIOBASE Biologic Database and RetNet to determine which of the candidate genes would be likely to

Table 2. Bio-information and biochemical assessment

Bio-information and blood test results	Normal range	Patient II-1	Patient II-2
Bio-information			
Weight (kg)		60	52
Height (m)		1.52	1.55
Body mass index (kg/m^2)	18.5–25	**25.96**	21.6
Biochemical assessment			
Fasting blood glucose (mg/dl)	65–109	**247**	77
Hemoglobin A1c (%)	4.6–6.2	**12.5**	6.0
Urea (mg/dl)	8–20	16	10
Creatinine (mg/dl)	0.50–1.10	0.99	0.63
Uric acid (mg/dl)	3.1–6.9	4.2	3.6
Sodium (mmol/l)	136–146	140	141
Potassium (mmol/l)	3.6–4.8	4.1	4.3
Chloride (mmol/l)	98–109	100	104
Calcium (mg/dl)	8.6–10.2	**10.3**	10.2
Aspartate aminotransferase (U/l)	10–33	**76**	**81**
Alanine aminotransferase (U/l)	6–35	**99**	**241**
Gamma glutamyl transpeptidase (U/l)	12–65	**134**	**135**
Alkaline phosphatase (U/l)	96–300	285	**319**
Low density lipoprotein-cholesterol (mg/dl)	70–139	120	**282**
Total cholesterol (mg/dl)	120–219	211	**441**
Triglycerides (mg/dl)	30–149	**309**	**761**
Albumin/globulin (g/dl)	3.5–5.2	5.0	5.1
Hemogram			
White blood cells (10^3/ml)	3.3–8.6	4.7	6.4
Red blood cells (10^6/ml)	4.10–5.50	5.00	4.88
Hemoglobin (g/dl)	13.5–16.5	14.0	14.3
Hematocrit (%)	40.0–50.0	42.3	42.7
Mean corpuscular volume (fl)	83.0–101.0	84.6	87.5
Platelets (10^3/ml)	150–350	166	251
Erythrocyte sedimentation rate (mm/h)	2–10	21	19
Hormones and autoantibodies			
Free T3 (pg/ml)	2.36–5.00	**2.34**	2.47
Free T4 (pmol/l)	0.88–1.67	1.33	**0.79**

Table 3. DNA sequence statistics

Family members	Read length (bp)	Number of reads	Mapping rate (%)	Mean depth (fold)	Coverage (%)
II-2 (younger brother)	101	47,724,724	99.4	46.6	88.5
II-1 (elder brother)	101	68,584,852	99.4	59.6	86.1
I-1 (father)	101	57,103,807	99.3	69.3	88.5
I-2 (mother)	101	59,776,264	99.3	56.8	86
Average	101	58,297,412	99.3	58.1	87.3

or anatomic changes of the retina [14,18,21,40] have been reported. For instance, a study of the pathology of the retina of a 2-year-old girl with AS showed hypocellularity of the ganglionic cell layer, the inner nuclear layer, and the outer nuclear layer (ONL) in addition to an absence of rod and cone outer segments and disruption of retinal pigment epithelium [18,21]; a study of a 42-year-old female with AS revealed severe reduction of all retinal layers containing a complete lack of photoreceptors and deposits of melanin pigments in the inner nuclear layer [14]; and OCT findings of a 5-year-old boy with AS showed only a slight thinning of the central retina [40]. In our patients, OCT findings showed marked retinal thinning (Figure 5A,B). The retinal layers of patient II-2 could not be distinguished because of marked retinal thinning (Figure 5C).

A study using retinal sections of *Almsl* knockout (*Almsl*$^{-/-}$) mice showed loss of the cell bodies in the ONL, shortening of the inner and outer segments, and incorrect localization of rhodopsin to the ONL [7]. The mislocalization of rhodopsin in the *Almsl*$^{-/-}$ mice indicates a defective rhodopsin transport system through the photoreceptor-connecting cilium [7]. The connecting cilium, damaged by loss of function of ALMS1, modifies the outer segments of the photoreceptors. Therefore, it has been suggested that defective protein transport across the connecting cilium is the probable cause of early onset severe retinal degeneration in AS patients [10]. We consider that the marked retinal thinning (Figure 5) and loss of retinal function (Figure 2) observed in our patients are due to a defective transport system across the photoreceptor-connecting cilium, resulting from the homozygous truncated mutation (p.Q2051X).

Variability in the phenotypic expression of AS is observed within sets of affected siblings [14,41–43]. Most patients with AS eventually develop T2DM, although there is wide variability in the age of onset [14]. Here, patient II-1 showed T2DM, but patient II-2 exhibited hyperinsulinemia, a predictor of T2DM (Table 2), suggesting that he might develop T2DM in the future. In addition, patient II-2 showed subclinical hypothyroidism, whereas patient II-1 did not exhibit hypothyroidism (Table 2). Hypothyroidism or subclinical hypothyroidism is reported to exist in approximately 20% of AS patients [14,19]. Most clinical features, such as retinal degeneration, hepatic dysfunction, hyperlipidemia, hypogonadism, short stature, and wide feet, were common features of the affected brothers (Table 1, Table 2); however, slight phenotypic differences in terms of glucose tolerance and thyroid function were observed between them.

ALMS1 protein has several notable sequence features, including an extensive tandem repeat domain (34×47 amino acid approximate tandem repeat, residues 538–2,199), a putative leucine-zipper motif (residues 2,480–2,501), and an ALMS motif (residues 4,035–4,167). Although the precise roles of the above domain and motifs are unknown, it is suggested that two regions of ALMS1—a relatively small internal region (residues 2,261–2,602) and a larger C-terminal region (residues 3,176–4,169)—play important

Table 4. Number of mutations after each filtering step

Filtering step	Number of mutations
1. Raw single-nucleotide variants plus *insertion–deletion* polymorphisms	3,506,741
2. Mutations capable of changing amino acid sequence	19,574
3. Mutations filtering by the snpEff score and existing at a frequency of less than 1% in 1000 genomes	3,685
4. Mutations filtering by the pattern of inheritance	17
5. Mutations expressed in retina, confirmed by SAGE database[a]	9
6. Mutations narrowed down using BIOBASE Biologic Database[b] and RetNet database[c]	1

[a]SAGE: serial analysis of gene expression;[b]BIOBASE Biologic Database (EyeSAGE); [c]RetNet database.

13. Marshall JD, Hinman EG, Collin GB, Beck S, Cerqueira R, Maffei P, Milan G, Zhang W, Wilson DI, Hearn T, Tavares P, Vettor R, Veronese C, Martin M, So WV, Nishina PM, Naggert JK. Spectrum of *ALMS1* variants and evaluation of genotype-phenotype correlations in Alström syndrome. Hum Mutat 2007; 28:1114-23. [PMID: 17594715].

14. Marshall JD, Bronson RT, Collin GB, Nordstrom AD, Maffei P, Paisey RB, Carey C, Macdermott S, Russell-Eggitt I, Shea SE, Davis J, Beck S, Shatirishvili G, Mihai CM, Hoeltzenbein M, Pozzan GB, Hopkinson I, Sicolo N, Naggert JK, Nishina PM. New Alström syndrome phenotypes based on the evaluation of 182 cases. Arch Intern Med 2005; 165:675-83. [PMID: 15795345].

15. Koç E, Bayrak G, Suher M, Ensari C, Aktas D, Ensari A. Rare case of Alström syndrome without obesity and with short stature, diagnosed in adulthood. Nephrology (Carlton) 2006; 11:81-4. [PMID: 16669965].

16. Akdeniz N, Bilgili SG, Aktar S, Yuca S, Calka O, Kilic A, Kosem M. Alström syndrome with acanthosis nigricans: a case report and literature review. Genet Couns 2011; 22:393-400. [PMID: 22303800].

17. Dyer DS, Wilson ME, Small KW, Pai GS. Alström syndrome: a case misdiagnosed as Bardet-Biedl syndrome. J Pediatr Ophthalmol Strabismus 1994; 31:272-4. [PMID: 7807310].

18. Russell-Eggitt IM, Clayton PT, Coffey R, Kriss A, Taylor DS, Taylor JF. Alström syndrome. Report of 22 cases and literature review. Ophthalmology 1998; 105:1274-80. [PMID: 9663233].

19. Marshall JD, Beck S, Maffei P, Naggert JK. Alström syndrome. Eur J Hum Genet 2007; 15:1193-202. [PMID: 17940554].

20. Lambert SR, Kriss A, Taylor D, Coffey R, Pembrey M. Follow-up and diagnostic reappraisal of 75 patients with Leber's congenital amaurosis. Am J Ophthalmol 1989; 107:624-31. [PMID: 2658617].

21. Russell-Eggitt IM, Taylor DS, Clayton PT, Garner A, Kriss A, Taylor JF. Leber's congenital amaurosis–a new syndrome with a cardiomyopathy. Br J Ophthalmol 1989; 73:250-4. [PMID: 2713302].

22. Ikeda Y, Morita Y, Matsuo Y, Akanuma Y, Itakura H. A case of Alström syndrome associated with situs inversus totalis and characteristic liver cirrhosis. Nippon Naika Gakkai Zasshi 1974; 63:1303-11. [PMID: 4477178].

23. Awazu M, Tanaka T, Sato S, Anzo M, Higuchi M, Yamazaki K, Matsuo N. Hepatic dysfunction in two sibs with Alström syndrome: case report and review of the literature. Am J Med Genet 1997; 69:13-6. [PMID: 9066877].

24. Awazu M, Tanaka T, Yamazaki K, Kato S, Higuchi M, Matsuo N. A 27-year-old woman with Alström syndrome who had liver cirrhosis. Keio J Med 1995; 44:67-73. [PMID: 7658647].

25. Shendure J, Ji H. Next-generation DNA sequencing. Nat Biotechnol 2008; 26:1135-45. [PMID: 18846087].

26. Mardis ER. The impact of next-generation sequencing technology on genetics. Trends Genet 2008; 24:133-41. [PMID: 18262675].

27. Mardis ER. Next-generation DNA sequencing methods. Annu Rev Genomics Hum Genet 2008; 9:387-402. [PMID: 18576944].

28. Ansorge WJ. Next-generation DNA sequencing techniques. New Biotechnol 2009; 25:195-203. [PMID: 19429539].

29. Teer JK, Mullikin JC. Exome sequencing: the sweet spot before whole genomes. Hum Mol Genet 2010; 19:R2R145-51. [PMID: 20705737].

30. Li Y, Vinckenbosch N, Tian G, Huerta-Sanchez E, Jiang T, Jiang H, Albrechtsen A, Andersen G, Cao H, Korneliussen T, Grarup N, Guo Y, Hellman I, Jin X, Li Q, Liu J, Liu X, Sparso T, Tang M, Wu H, Wu R, Yu C, Zheng H, Astrup A, Bolund L, Holmkvist J, Jorgensen T, Kristiansen K, Schmitz O, Schwartz TW, Zhang X, Li R, Yang H, Wang J, Hansen T, Pedersen O, Nielsen R, Wang J. Resequencing of 200 human exomes identifies an excess of low-frequency non-synonymous coding variants. Nat Genet 2010; 42:969-72. [PMID: 20890277].

31. Kim DW, Nam SH, Kim RN, Choi SH, Park HS. Whole human exome capture for high-throughput sequencing. Genome 2010; 53:568-74. [PMID: 20616878].

32. Hodges E, Rooks M, Xuan Z, Bhattacharjee A, Benjamin Gordon D, Brizuela L, Richard McCombie W, Hannon GJ. Hybrid selection of discrete genomic intervals on custom-designed microarrays for massively parallel sequencing. Nat Protoc 2009; 4:960-74. [PMID: 19478811].

33. Takeuchi T, Hayashi T, Bedell M, Zhang K, Yamada H, Tsuneoka H. A novel haplotype with the R345W mutation in the EFEMP1 gene associated with autosomal dominant drusen in a Japanese family. Invest Ophthalmol Vis Sci 2010; 51:1643-50. [PMID: 19850834].

34. Li H, Durbin R. Fast and accurate short read alignment with Burrows-Wheeler transform. Bioinformatics 2009; 25:1754-60. [PMID: 19451168].

35. McKenna A, Hanna M, Banks E, Sivachenko A, Cibulskis K, Kernytsky A, Garimella K, Altshuler D, Gabriel S, Daly M, DePristo MA. The Genome Analysis Toolkit: a MapReduce framework for analyzing next-generation DNA sequencing data. Genome Res 2010; 20:1297-303. [PMID: 20644199].

36. Cingolani P, Platts A, Wang le L, Coon M, Nguyen T, Wang L, Land SJ, Lu X, Ruden DM. A program for annotating and predicting the effects of single nucleotide polymorphisms, SnpEff: SNPs in the genome of Drosophila melanogaster strain w1118; iso-2; iso-3. Fly (Austin) 2012; 6:80-92. [PMID: 22728672].

37. Adzhubei I, Jordan DM, Sunyaev SR. Predicting functional effect of human missense mutations using PolyPhen-2. Curr Protoc Hum Genet 2013; Chapter 7:Unit7 20.

38. Green JS, Parfrey PS, Harnett JD, Farid NR, Cramer BC, Johnson G, Heath O, McManamon PJ, O'Leary E, Pryse-Phillips W. The cardinal manifestations of Bardet-Biedl syndrome, a form of Laurence-Moon-Biedl syndrome. N Engl J Med 1989; 321:1002-9. [PMID: 2779627].

Clinical Ophthalmology Dove

CASE REPORT

Two siblings with late-onset cone–rod dystrophy and no visible macular degeneration

Hiroyuki Sakuramoto[1]
Kazuki Kuniyoshi[1]
Kazushige Tsunoda[2]
Masakazu Akahori[2]
Takeshi Iwata[2]
Yoshikazu Shimomura[1]

[1]Department of Ophthalmology, Kinki University Faculty of Medicine, Osaka-Sayama City, Osaka, Japan; [2]National Institute of Sensory Organs, National Hospital Organization Tokyo Medical Center, Tokyo, Japan

Background: We report our findings in two siblings with late-onset cone–rod dystrophy (CRD) with no visible macular degeneration.

Cases and methods: Case 1 was an 82-year-old man who first noticed a decrease in vision and color blindness in his early seventies. His mother and younger sister also had visual disturbances. His decimal visual acuity was 0.3 in the right eye and 0.2 in the left eye. Ophthalmoscopy showed normal fundi, and fluorescein angiography was also normal in both eyes. The photopic single flash and flicker eletroretinograms (ERGs) were severely attenuated and the scotopic ERGs were slightly reduced in both eyes. Case 2 was the 80-year-old younger sister of Case 1. She first noticed a decline in vision and photophobia in both eyes in her early seventies. Her decimal visual acuity was 0.4 in the right eye and 0.2 in the left eye. Ophthalmoscopy showed mottling of the retinal pigment epithelium in the midperiphery with no visible macular degeneration. The photopic single flash and flicker ERGs were severely attenuated, and the scotopic ERGs were slightly reduced in both eyes.

Conclusion: These siblings are the oldest reported cases of CRD with no visible macular degeneration. Thus, CRD should be considered in patients with reduced visual acuity, color blindness, and photophobia even if they are older than 70 years.

Keywords: cone–rod dystrophy, peripheral cone dystrophy, occult macular dystrophy, late onset, macular degeneration, negative ERG

Introduction

Cone–rod dystrophy (CRD) is an inherited retinal dystrophy that is characterized by reduced visual acuity, color blindness, and photophobia.[1–3] The age of onset generally ranges from the teens to the thirties,[2,3] and most patients with CRD have atrophic macular degeneration with a bull's eye lesion, or midperipheral degeneration in the late stages of the disease.[2,3] Patients with CRD can also have a central scotoma, and constriction of the peripheral visual fields at the end stages of the disease.[2,3] The cone-driven electroretinograms (ERGs) are attenuated even in the early stages, and this reduction is essential for making a diagnosis of CRD.[2,3]

Cases of atypical CRD, such as CRD with normal fundi,[4–7] occult macular dystrophy (OMD; Miyake disease),[8–11] peripheral cone dystrophy,[12–15] fundus albipunctatus associated with cone dystrophy,[16,17] and cone dystrophy with supernormal rod ERGs[18,19] have also been reported.

We present the clinical features of two siblings with CRD who had only mild fundus abnormalities. Their mother was also known to have visual difficulties, but was already dead at the time the two siblings were examined.

Correspondence: Kazuki Kuniyoshi
Department of Ophthalmology, Kinki University Faculty of Medicine, 377-2 Ohno-Higashi, Osaka-Sayama City, Osaka 589-8511, Japan
Tel +81 723 660 221
Fax +81 723 682 559
Email kazuki@med.kindai.ac.jp

Cases and methods

Our two cases were siblings who underwent ophthalmoscopy, visual acuity measurements, fundus fluorescein angiography (FA), Goldmann kinetic perimetry, Farnsworth D-15 test, Goldmann–Weekers dark adaptometry, full-field ERGs, multifocal ERGs (mfERGs), and optical coherence tomography (OCT). OCT images recorded from 24 age-matched normal subjects served as controls.

The ERGs and mfERGs were recorded according to the protocol recommended by the International Society for Clinical Electrophysiology of Vision. The mfERGs were recorded with the VERIS™ recording system (Electro-Diagnostic Imaging, Inc, Redwood, CA, USA). A Cirrus™ high-definition spectral-domain OCT instrument (Carl Zeiss Meditec AG, Jena, Germany) was used to obtain the OCT images.

Case reports

Case 1 was an 82-year-old man who first noticed a decrease in his vision and color vision in both eyes in his early seventies. His decimal best-corrected visual acuity (BCVA) at our initial examination was 0.3 oculus dexter (OD) with +3.25 diopters (D) and 0.2 oculus sinister (OS) with +3.25 D. His pupillary light reflexes and intraocular pressures were normal in both eyes. There was no history of the use of retinotoxic drugs. His cataracts were removed in both eyes at age 75; however, his vision was not improved.

Ophthalmoscopy showed that the fundus was normal in both eyes, and FA showed small hyperfluorescent spots at the parafoveal region of the left eye (Figure 1). Goldmann kinetic perimetry showed a central scotoma in both eyes (Figure 2), and Farnsworth D-15 test showed a tritan axis error. Goldmann–Weekers dark adaptometry revealed a slight elevation of the threshold in both eyes (Figure 3). The full-field scotopic ERGs elicited by both low- and high-intensity stimuli were slightly reduced. The scotopic b-wave elicited by a high-intensity stimulus was smaller than the a-wave, resulting in a negative-type ERG (Figure 4). On the other hand, photopic single-flash and 30 Hz flicker ERGs were severely attenuated in both eyes (Figure 4). The mfERGs were

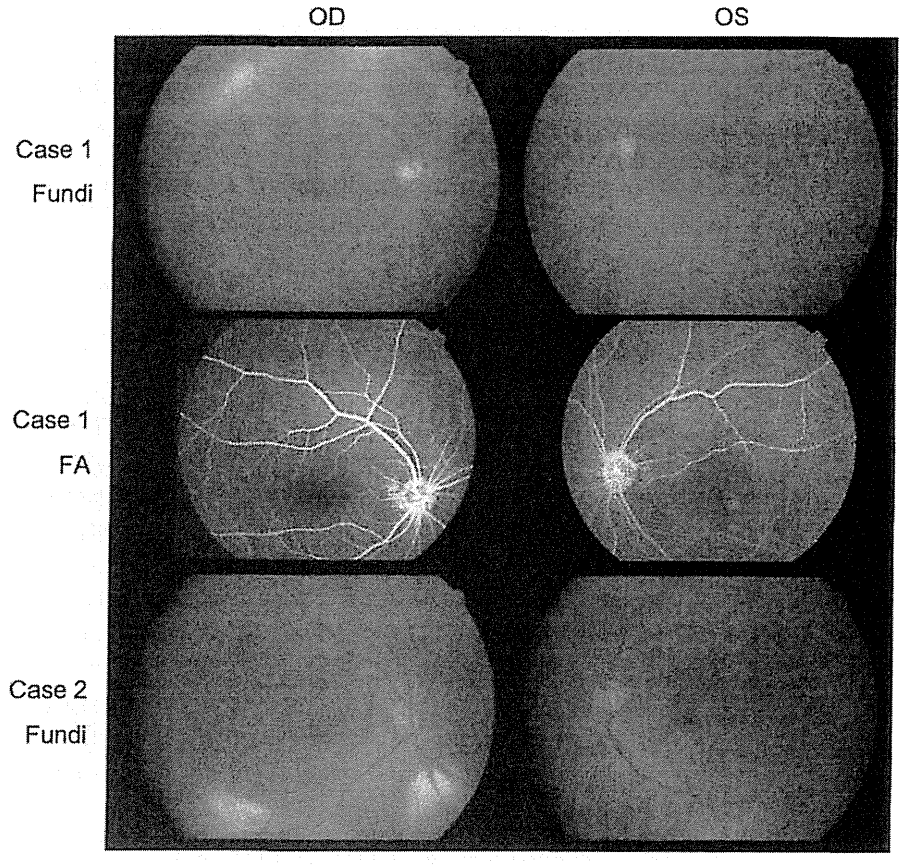

Figure 1 Fundus photographs (Fundi) and FA.
Abbreviations: OD, oculus dexter; OS, oculus sinister; FA, fluorescein fundus angiograms.

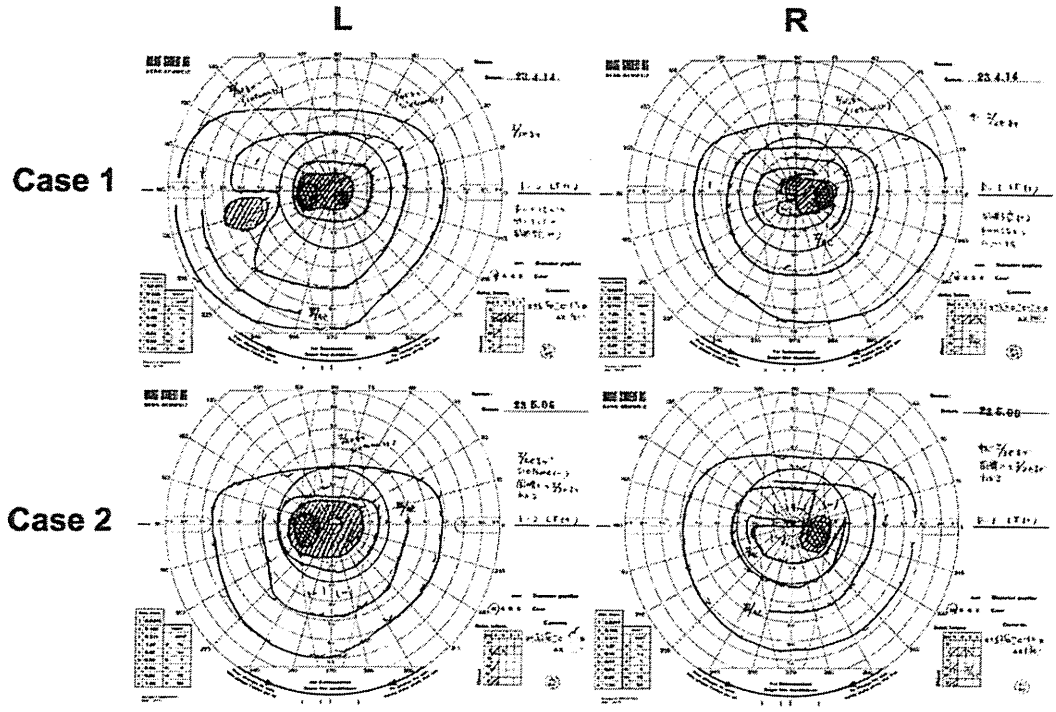

Figure 2 Results of Goldmann kinetic perimetry.
Abbreviations: L, left; R, right.

nonrecordable in the central area, but small responses were recorded in the midperiphery (Figure 5). The photoreceptor inner segment/outer segment junction line was indistinct in the OCT images (Figure 6). The thickness of the outer nuclear layer was 76 µm OD and 65 µm OS (normal mean 172 ± 17 µm) at the fovea, 65 µm OD and 43 µm OS (normal mean 128 ± 19 µm) at 0.5 mm superior to the fovea, and 65 µm OD and 54 µm OS (normal mean 135 ± 23 µm) at 0.5 mm inferior to the fovea. At 2 mm superior to the fovea, the thickness of the outer nuclear layer was 65 µm OD and 43 µm OS (normal mean 97 ± 13 µm), and at 2 mm inferior to the fovea it was 43 µm OD and 54 µm OS (normal

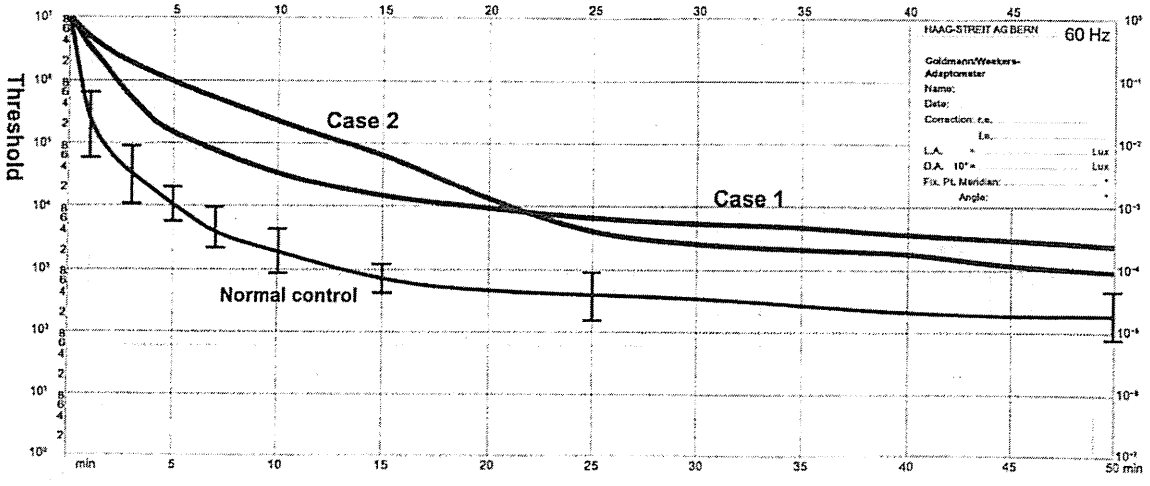

Figure 3 Results of Goldmann–Weekers dark adaptometry.
Note: The thin line indicates the average ± standard deviation isopter of normal controls.

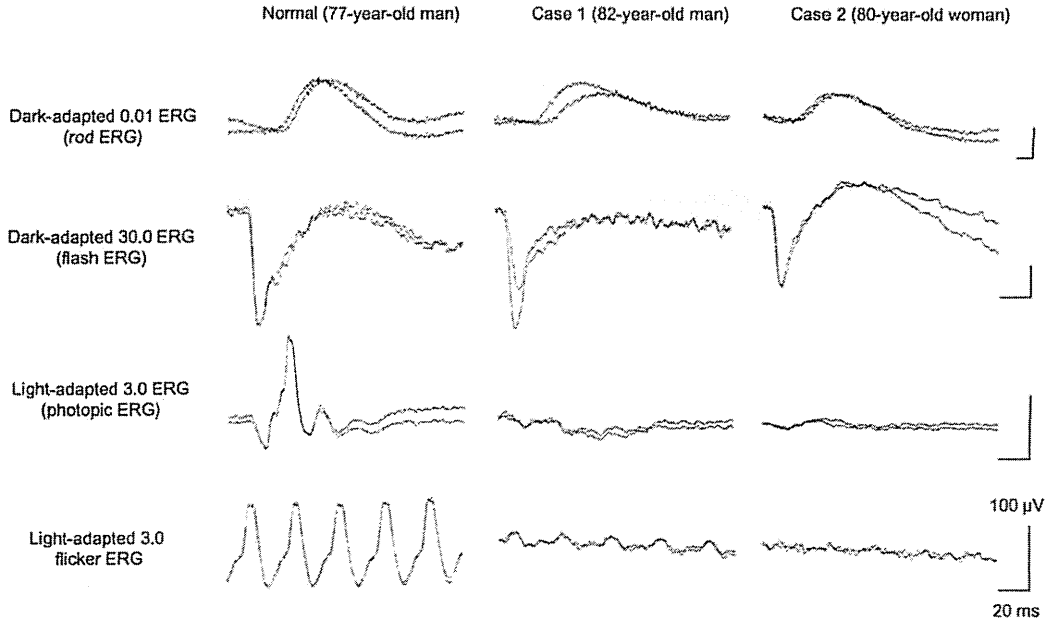

Figure 4 International Society for Clinical Electrophysiology of Vision-standard ERGs.
Note: The responses from both eyes are superimposed.
Abbreviation: ERG, electroretinography.

mean 88 ± 18 μm). Thus, the outer nuclear layer was thin, especially in the parafoveal region in both eyes (Figure 6). The thickness of the middle and inner layers of the retina were within normal limits.

Case 2 was the younger sister of case 1. She was 80 years old and had first noticed a decrease in her vision and photophobia in both eyes in her early seventies. Her cataract was removed in both eyes at age 76; however, her vision was not improved.

Our examination showed that her decimal BCVA was 0.4 OD with +0.25 D and 0.2 OS with +0.5 D. Her pupillary light reflexes and intraocular pressures were normal in both eyes. There was no history of retinotoxic drug use.

Her fundus was normal except for a slight mottling of the retinal pigment epithelium in the midperiphery. No macular degeneration was seen in either eye (Figure 1). FA was not performed because of her allergy to fluorescein sodium. Goldmann kinetic perimetry revealed a central scotoma in the left eye and a mild constriction of the visual fields in both eyes (Figure 2). Farnsworth D-15 test showed tritan axis errors in both eyes. Goldmann–Weekers dark adaptometry showed a slight elevation of the light threshold in both eyes (Figure 3). The full-field scotopic ERGs elicited by low-intensity stimuli were slightly reduced, and the scotopic high-intensity ERGs were normal, except the oscillatory potentials were reduced. The photopic single-flash and 30 Hz flicker ERGs were nonrecordable in both eyes (Figure 4). The mfERGs were nonrecordable in the right eye and reduced in the central and midperipheral areas of the left eye (Figure 5). OCT showed similar findings to her elder brother in the macular area (Figure 6). The photoreceptor inner segment/outer segment junction line was indistinct. The thickness of the outer nuclear layer was 130 μm OD and 129 μm OS (normal mean 172 ± 17 μm) at the fovea, 43 μm OD and 65 μm OS (normal mean 128 ± 19 μm) at 0.5 mm superior to the fovea, and 32 μm OD and 22 μm OS (normal mean 135 ± 23 μm) at 0.5 mm inferior to the fovea. At 2 mm superior to the fovea, the thickness of the outer nuclear layer was 65 μm OD and 76 μm OS (normal mean 97 ± 13 μm), and at 2 mm inferior to the fovea it was 65 μm OD and 43 μm OS (normal mean 88 ± 18 μm). Thus, the outer nuclear layer was thin, especially in the parafoveal region of both eyes (Figure 6).

Discussion

These two high-aged siblings, both in their eighties, had severely attenuated cone ERGs and mfERGs, and there was no evidence of visible macular abnormality. Case 1 had small hyperfluorescent spots in the fluorescein angiograms, and case 2 had mottling in the midperipheral fundus. Goldmann kinetic perimetry showed a central scotoma and reduced sensitivity in the area surrounding the scotoma in both patients. The mfERGs were nonrecordable in the foveal area, and only

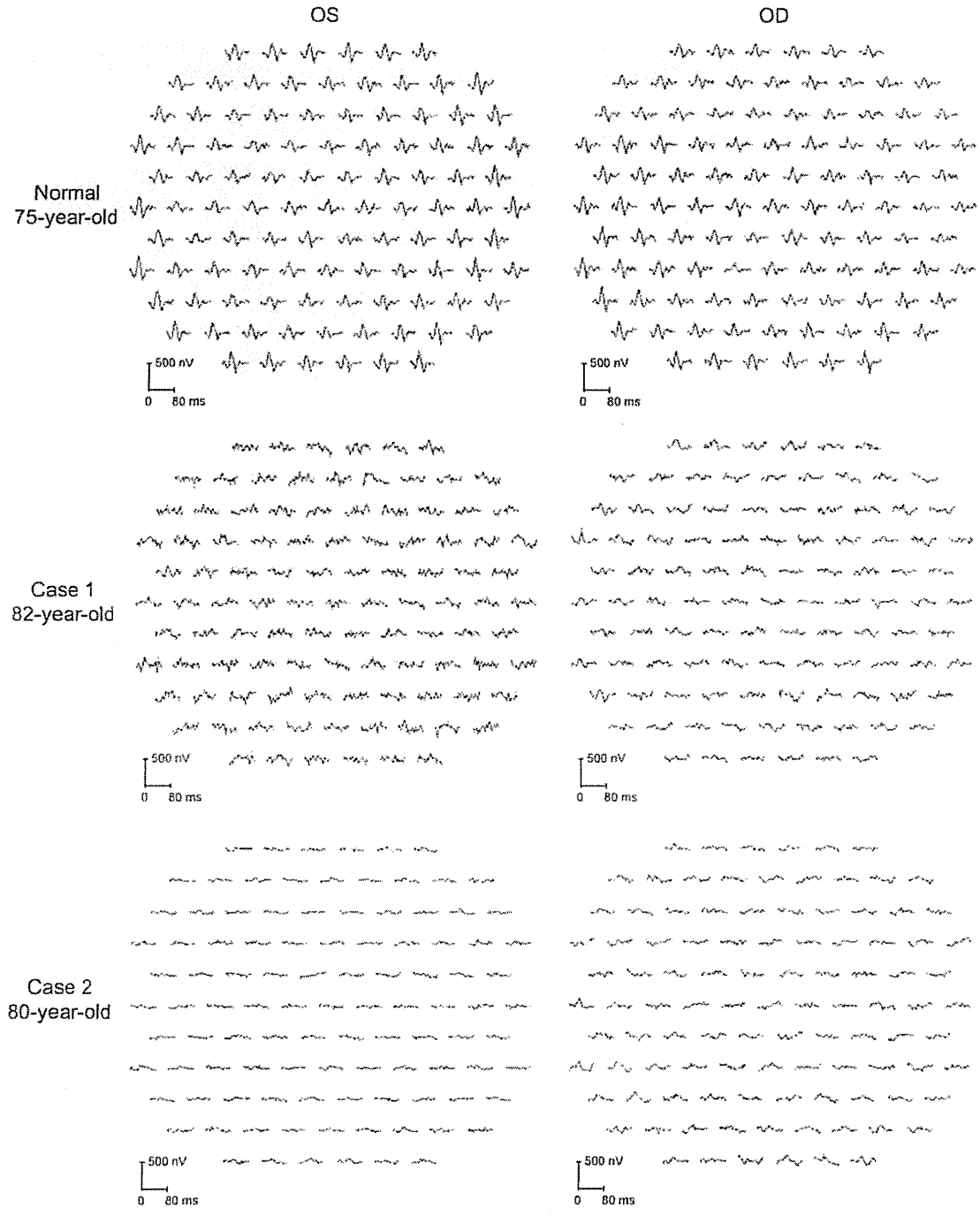

Figure 5 Multifocal ERGs.
Note: Responses were contaminated with much noise which was caused by photophobia.
Abbreviations: OS, oculus sinister; OD, oculus dexter; ERG, electroretinography.

very small responses were recorded in the midperiphery; these findings are consistent with results of the Goldmann kinetic perimetry.

We reviewed 497 CRD cases in 181 papers. Among these, 86 eyes in 43 patients in 20 papers were reported to have either normal fundus or only subtle fundus abnormalities (Figure 7).[4–7,20–35]

The vision of these cases is summarized in Figure 7, and the findings suggested that the vision in CRD cases with normal fundi is better than that in CRD cases with